

Study of the Baryon-Antibaryon Low-Mass Enhancements in Charmless Three-body Baryonic B Decays

K. Abe,¹⁰ K. Abe,⁴⁶ N. Abe,⁴⁹ I. Adachi,¹⁰ H. Aihara,⁴⁸ M. Akatsu,²⁴ Y. Asano,⁵³
 T. Aso,⁵² V. Aulchenko,² T. Aushev,¹⁴ T. Aziz,⁴⁴ S. Bahinipati,⁶ A. M. Bakich,⁴³
 Y. Ban,³⁶ M. Barbero,⁹ A. Bay,²⁰ I. Bedny,² U. Bitenc,¹⁵ I. Bizjak,¹⁵ S. Blyth,²⁹
 A. Bondar,² A. Bozek,³⁰ M. Bračko,^{22,15} J. Brodzicka,³⁰ T. E. Browder,⁹ M.-C. Chang,²⁹
 P. Chang,²⁹ Y. Chao,²⁹ A. Chen,²⁶ K.-F. Chen,²⁹ W. T. Chen,²⁶ B. G. Cheon,⁴
 R. Chistov,¹⁴ S.-K. Choi,⁸ Y. Choi,⁴² Y. K. Choi,⁴² A. Chuvikov,³⁷ S. Cole,⁴³
 M. Danilov,¹⁴ M. Dash,⁵⁵ L. Y. Dong,¹² R. Dowd,²³ J. Dragic,²³ A. Drutskoy,⁶
 S. Eidelman,² Y. Enari,²⁴ D. Epifanov,² C. W. Everton,²³ F. Fang,⁹ S. Fratina,¹⁵
 H. Fujii,¹⁰ N. Gabyshev,² A. Garmash,³⁷ T. Gershon,¹⁰ A. Go,²⁶ G. Gokhroo,⁴⁴
 B. Golob,^{21,15} M. Grosse Perdekamp,³⁸ H. Guler,⁹ J. Haba,¹⁰ F. Handa,⁴⁷ K. Hara,¹⁰
 T. Hara,³⁴ N. C. Hastings,¹⁰ K. Hasuko,³⁸ K. Hayasaka,²⁴ H. Hayashii,²⁵ M. Hazumi,¹⁰
 E. M. Heenan,²³ I. Higuchi,⁴⁷ T. Higuchi,¹⁰ L. Hinz,²⁰ T. Hojo,³⁴ T. Hokuue,²⁴
 Y. Hoshi,⁴⁶ K. Hoshina,⁵¹ S. Hou,²⁶ W.-S. Hou,²⁹ Y. B. Hsiung,²⁹ H.-C. Huang,²⁹
 T. Igaki,²⁴ Y. Igarashi,¹⁰ T. Iijima,²⁴ A. Imoto,²⁵ K. Inami,²⁴ A. Ishikawa,¹⁰ H. Ishino,⁴⁹
 K. Itoh,⁴⁸ R. Itoh,¹⁰ M. Iwamoto,³ M. Iwasaki,⁴⁸ Y. Iwasaki,¹⁰ R. Kagan,¹⁴ H. Kakuno,⁴⁸
 J. H. Kang,⁵⁶ J. S. Kang,¹⁷ P. Kapusta,³⁰ S. U. Kataoka,²⁵ N. Katayama,¹⁰ H. Kawai,³
 H. Kawai,⁴⁸ Y. Kawakami,²⁴ N. Kawamura,¹ T. Kawasaki,³² N. Kent,⁹ H. R. Khan,⁴⁹
 A. Kibayashi,⁴⁹ H. Kichimi,¹⁰ H. J. Kim,¹⁹ H. O. Kim,⁴² Hyunwoo Kim,¹⁷ J. H. Kim,⁴²
 S. K. Kim,⁴¹ T. H. Kim,⁵⁶ K. Kinoshita,⁶ P. Koppenburg,¹⁰ S. Korpar,^{22,15} P. Križan,^{21,15}
 P. Krokovny,² R. Kulasiri,⁶ C. C. Kuo,²⁶ H. Kurashiro,⁴⁹ E. Kurihara,³ A. Kusaka,⁴⁸
 A. Kuzmin,² Y.-J. Kwon,⁵⁶ J. S. Lange,⁷ G. Leder,¹³ S. E. Lee,⁴¹ S. H. Lee,⁴¹
 Y.-J. Lee,²⁹ T. Lesiak,³⁰ J. Li,⁴⁰ A. Limosani,²³ S.-W. Lin,²⁹ D. Liventsev,¹⁴
 J. MacNaughton,¹³ G. Majumder,⁴⁴ F. Mandl,¹³ D. Marlow,³⁷ T. Matsuishi,²⁴
 H. Matsumoto,³² S. Matsumoto,⁵ T. Matsumoto,⁵⁰ A. Matyja,³⁰ Y. Mikami,⁴⁷
 W. Mitaroff,¹³ K. Miyabayashi,²⁵ Y. Miyabayashi,²⁴ H. Miyake,³⁴ H. Miyata,³² R. Mizuk,¹⁴
 D. Mohapatra,⁵⁵ G. R. Moloney,²³ G. F. Moorhead,²³ T. Mori,⁴⁹ A. Murakami,³⁹
 T. Nagamine,⁴⁷ Y. Nagasaka,¹¹ T. Nakadaira,⁴⁸ I. Nakamura,¹⁰ E. Nakano,³³ M. Nakao,¹⁰
 H. Nakazawa,¹⁰ Z. Natkaniec,³⁰ K. Neichi,⁴⁶ S. Nishida,¹⁰ O. Nitoh,⁵¹ S. Noguchi,²⁵
 T. Nozaki,¹⁰ A. Ogawa,³⁸ S. Ogawa,⁴⁵ T. Ohshima,²⁴ T. Okabe,²⁴ S. Okuno,¹⁶
 S. L. Olsen,⁹ Y. Onuki,³² W. Ostrowicz,³⁰ H. Ozaki,¹⁰ P. Pakhlov,¹⁴ H. Palka,³⁰
 C. W. Park,⁴² H. Park,¹⁹ K. S. Park,⁴² N. Parslow,⁴³ L. S. Peak,⁴³ M. Pernicka,¹³
 J.-P. Perroud,²⁰ M. Peters,⁹ L. E. Piilonen,⁵⁵ A. Poluektov,² F. J. Ronga,¹⁰ N. Root,²
 M. Rozanska,³⁰ H. Sagawa,¹⁰ M. Saigo,⁴⁷ S. Saitoh,¹⁰ Y. Sakai,¹⁰ H. Sakamoto,¹⁸
 T. R. Sarangi,¹⁰ M. Satapathy,⁵⁴ N. Sato,²⁴ O. Schneider,²⁰ J. Schümann,²⁹ C. Schwanda,¹³
 A. J. Schwartz,⁶ T. Seki,⁵⁰ S. Semenov,¹⁴ K. Senyo,²⁴ Y. Settai,⁵ R. Seuster,⁹
 M. E. Sevier,²³ T. Shibata,³² H. Shibuya,⁴⁵ B. Shwartz,² V. Sidorov,² V. Siegle,³⁸
 J. B. Singh,³⁵ A. Somov,⁶ N. Soni,³⁵ R. Stamen,¹⁰ S. Stanič,^{53,*} M. Starič,¹⁵ A. Sugi,²⁴
 A. Sugiyama,³⁹ K. Sumisawa,³⁴ T. Sumiyoshi,⁵⁰ S. Suzuki,³⁹ S. Y. Suzuki,¹⁰ O. Tajima,¹⁰
 F. Takasaki,¹⁰ K. Tamai,¹⁰ N. Tamura,³² K. Tanabe,⁴⁸ M. Tanaka,¹⁰ G. N. Taylor,²³

arXiv:hep-ex/0409010v1 2 Sep 2004

Y. Teramoto,³³ X. C. Tian,³⁶ S. Tokuda,²⁴ S. N. Tovey,²³ K. Trabelsi,⁹ T. Tsuboyama,¹⁰
T. Tsukamoto,¹⁰ K. Uchida,⁹ S. Uehara,¹⁰ T. Uglov,¹⁴ K. Ueno,²⁹ Y. Unno,³ S. Uno,¹⁰
Y. Ushiroda,¹⁰ G. Varner,⁹ K. E. Varvell,⁴³ S. Villa,²⁰ C. C. Wang,²⁹ C. H. Wang,²⁸
J. G. Wang,⁵⁵ M.-Z. Wang,²⁹ M. Watanabe,³² Y. Watanabe,⁴⁹ L. Widhalm,¹³
Q. L. Xie,¹² B. D. Yabsley,⁵⁵ A. Yamaguchi,⁴⁷ H. Yamamoto,⁴⁷ S. Yamamoto,⁵⁰
T. Yamanaka,³⁴ Y. Yamashita,³¹ M. Yamauchi,¹⁰ Heyoung Yang,⁴¹ P. Yeh,²⁹ J. Ying,³⁶
K. Yoshida,²⁴ Y. Yuan,¹² Y. Yusa,⁴⁷ H. Yuta,¹ S. L. Zang,¹² C. C. Zhang,¹² J. Zhang,¹⁰
L. M. Zhang,⁴⁰ Z. P. Zhang,⁴⁰ V. Zhilich,² T. Ziegler,³⁷ D. Žontar,^{21,15} and D. Zürcher²⁰

(The Belle Collaboration)

¹*Aomori University, Aomori*

²*Budker Institute of Nuclear Physics, Novosibirsk*

³*Chiba University, Chiba*

⁴*Chonnam National University, Kwangju*

⁵*Chuo University, Tokyo*

⁶*University of Cincinnati, Cincinnati, Ohio 45221*

⁷*University of Frankfurt, Frankfurt*

⁸*Gyeongsang National University, Chinju*

⁹*University of Hawaii, Honolulu, Hawaii 96822*

¹⁰*High Energy Accelerator Research Organization (KEK), Tsukuba*

¹¹*Hiroshima Institute of Technology, Hiroshima*

¹²*Institute of High Energy Physics,*

Chinese Academy of Sciences, Beijing

¹³*Institute of High Energy Physics, Vienna*

¹⁴*Institute for Theoretical and Experimental Physics, Moscow*

¹⁵*J. Stefan Institute, Ljubljana*

¹⁶*Kanagawa University, Yokohama*

¹⁷*Korea University, Seoul*

¹⁸*Kyoto University, Kyoto*

¹⁹*Kyungpook National University, Taegu*

²⁰*Swiss Federal Institute of Technology of Lausanne, EPFL, Lausanne*

²¹*University of Ljubljana, Ljubljana*

²²*University of Maribor, Maribor*

²³*University of Melbourne, Victoria*

²⁴*Nagoya University, Nagoya*

²⁵*Nara Women's University, Nara*

²⁶*National Central University, Chung-li*

²⁷*National Kaohsiung Normal University, Kaohsiung*

²⁸*National United University, Miao Li*

²⁹*Department of Physics, National Taiwan University, Taipei*

³⁰*H. Niewodniczanski Institute of Nuclear Physics, Krakow*

³¹*Nihon Dental College, Niigata*

³²*Niigata University, Niigata*

³³*Osaka City University, Osaka*

³⁴*Osaka University, Osaka*

³⁵*Panjab University, Chandigarh*

³⁶*Peking University, Beijing*

- ³⁷*Princeton University, Princeton, New Jersey 08545*
³⁸*RIKEN BNL Research Center, Upton, New York 11973*
³⁹*Saga University, Saga*
⁴⁰*University of Science and Technology of China, Hefei*
⁴¹*Seoul National University, Seoul*
⁴²*Sungkyunkwan University, Suwon*
⁴³*University of Sydney, Sydney NSW*
⁴⁴*Tata Institute of Fundamental Research, Bombay*
⁴⁵*Toho University, Funabashi*
⁴⁶*Tohoku Gakuin University, Tagajo*
⁴⁷*Tohoku University, Sendai*
⁴⁸*Department of Physics, University of Tokyo, Tokyo*
⁴⁹*Tokyo Institute of Technology, Tokyo*
⁵⁰*Tokyo Metropolitan University, Tokyo*
⁵¹*Tokyo University of Agriculture and Technology, Tokyo*
⁵²*Toyama National College of Maritime Technology, Toyama*
⁵³*University of Tsukuba, Tsukuba*
⁵⁴*Utkal University, Bhubaneswer*
⁵⁵*Virginia Polytechnic Institute and State University, Blacksburg, Virginia 24061*
⁵⁶*Yonsei University, Seoul*

Abstract

The angular distributions of the baryon-antibaryon low-mass enhancements seen in the charmless three-body baryonic B decays $B^+ \rightarrow p\bar{p}K^+$, $B^0 \rightarrow p\bar{p}K_S^0$, and $B^0 \rightarrow p\bar{\Lambda}\pi^-$ are reported. Searches for the pentaquarks Θ^+ and Θ^{++} in the relevant decay modes and possible glueball states in the $p\bar{p}$ systems are presented. The analysis is based on a 140 fb^{-1} data sample recorded on the $\Upsilon(4S)$ resonance with the Belle detector at the KEKB asymmetric-energy e^+e^- collider.

PACS numbers: 13.25.Hw, 13.60.Rj

Observations of several baryonic three-body B decays have been reported recently [1, 2, 3]. One common feature of these observations is the peaking of the baryon-antibaryon pair mass spectra toward threshold, as originally conjectured in Refs. [4, 5] and elaborated more recently in Refs. [6, 7, 8]. The same peaking behavior near threshold has been found in J/ψ decays [9] as well, indicating that this might be a universal phenomenon. The possible explanations include the presence of intermediate gluonic states or side effects of the quark fragmentation process. Alternatively, the dynamical picture can be replaced by an effective range analysis with a baryon form factor. To distinguish among the above production mechanism hypotheses, we study the threshold enhancements by examining the angular distributions in the helicity frame for the $p\bar{p}K^+$, $p\bar{p}K_S^0$ and $p\bar{\Lambda}\pi^-$ [10] modes. Also, we update the mass spectra from our previous studies.

We use a 140 fb^{-1} data sample, consisting of $152 \times 10^6 B\bar{B}$ pairs, collected by the Belle detector at the KEKB asymmetric energy e^+e^- (3.5 on 8 GeV) collider [11]. The Belle detector is a large solid angle magnetic spectrometer that consists of a three layer silicon vertex detector (SVD), a 50 layer central drift chamber (CDC), an array of aerogel threshold Čerenkov counters (ACC), a barrel-like arrangement of time of flight scintillation counters (TOF), and an electromagnetic calorimeter comprised of CsI(Tl) crystals located inside a superconducting solenoid coil that provides a 1.5 T magnetic field. An iron flux return located outside of the coil is instrumented to detect K_L^0 mesons and to identify muons. The detector is described in detail elsewhere [12].

The event selection criteria are based on the information obtained from the tracking system (SVD+CDC) and the hadron identification system (CDC+ACC+TOF). All primary charged tracks are required to satisfy track quality criteria based on the track impact parameters relative to the interaction point (IP). The deviations from the IP position are required to be within ± 1 cm in the transverse (x - y) plane, and within ± 3 cm in the z direction, where the z axis is opposite the positron beam line. For each track, the likelihood values L_p , L_K , and L_π that it is a proton, kaon, or pion, respectively, are determined from the information provided by the hadron identification system. The track is identified as a proton if $L_p/(L_p + L_K) > 0.6$ and $L_p/(L_p + L_\pi) > 0.6$, or as a kaon if $L_K/(L_K + L_\pi) > 0.6$, or as a pion if $L_\pi/(L_K + L_\pi) > 0.6$. Candidate K_S^0 mesons are reconstructed from pairs of oppositely charged tracks (both treated as pions) having an invariant mass consistent with the K_S^0 nominal mass, as well as a displaced vertex and flight direction consistent with an origin at the IP. A candidate Λ baryon is reconstructed from a pair of oppositely charged tracks—treated as a proton and negative pion—whose invariant mass is consistent with the nominal Λ baryon mass. The proton-like daughter is required to satisfy $L_p/(L_p + L_\pi) > 0.6$.

Candidate B mesons are reconstructed from the related final state particles for the $B^+ \rightarrow p\bar{p}K^+$, $B^0 \rightarrow p\bar{p}K_S^0$, and $B^0 \rightarrow p\bar{\Lambda}\pi^-$ modes. We use two kinematic variables in the center of mass (CM) frame to identify the reconstructed B meson candidates: the beam energy constrained mass $M_{bc} = \sqrt{E_{\text{beam}}^2 - p_B^2}$, and the energy difference $\Delta E = E_B - E_{\text{beam}}$, where E_{beam} is the beam energy, and p_B and E_B are the momentum and energy, respectively, of the reconstructed B meson. The fit region is defined as $5.20 \text{ GeV}/c^2 < M_{bc} < 5.29 \text{ GeV}/c^2$ and $-0.1 \text{ GeV} < \Delta E < 0.2 \text{ GeV}$. From a GEANT based Monte Carlo (MC) simulation, the signal peaks in the subregion $5.27 \text{ GeV}/c^2 < M_{bc} < 5.29 \text{ GeV}/c^2$ and $|\Delta E| < 0.05 \text{ GeV}$. The lower bound of ΔE is chosen to exclude possible contamination from so-called “cross-feed” baryonic B decays.

The background in the fit region solely arises from the continuum $e^+e^- \rightarrow q\bar{q}$ ($q = u, d, s, c$) process. We suppress the jet-like continuum background events relative to the

more spherical $B\bar{B}$ signal events using a Fisher discriminant [13] that combines seven event shape variables, as described in Ref. [14]. Probability density functions (PDFs) for the Fisher discriminant and the cosine of the angle between the B flight direction and the beam direction in the $\Upsilon(4S)$ rest frame are combined to form the signal (background) likelihood \mathcal{L}_s (\mathcal{L}_b). The signal PDFs are determined using signal MC simulation; the background PDFs are obtained from the side-band data with $M_{bc} < 5.26$ GeV/ c^2 . We require the likelihood ratio $\mathcal{R} = \mathcal{L}_s/(\mathcal{L}_s + \mathcal{L}_b)$ to be greater than 0.7, 0.75, and 0.8 for the $p\bar{p}K^+$, $p\bar{p}K_S^0$, and $p\bar{\Lambda}\pi^-$ modes, respectively. These selection criteria are determined by optimization of $n_s/\sqrt{n_s + n_b}$, where n_s and n_b denote the expected numbers of signal and background events, respectively. We use the branching fractions from our previous measurements [1, 2, 3] in the calculation of n_s . If there are multiple B candidates in one event, we select the one with the best χ^2 value from the B meson vertex fit, in which only the primary charged tracks are used. Based on previous studies [1, 2, 3], we require the invariant mass of the baryon pair to be less than 2.85 GeV/ c^2 for the study of the threshold enhancement effect that follows.

The M_{bc} distributions (with $|\Delta E| < 0.05$ GeV), and the ΔE distributions (with $M_{bc} > 5.27$ GeV/ c^2) for the $p\bar{p}K^+$, $p\bar{p}K_S^0$ and $p\bar{\Lambda}\pi^-$ modes are shown in Fig. 1. We use an unbinned likelihood fit that maximize the likelihood function,

$$L = \frac{e^{-(N_s+N_b)}}{N!} \prod_{i=1}^N \left[N_s P_s(M_{bc_i}, \Delta E_i) + N_b P_b(M_{bc_i}, \Delta E_i) \right],$$

to estimate the signal yield; here P_s (P_b) denotes the signal (background) PDF, N is the number of events in the fit, and N_s and N_b are free parameters representing the number of signal and background events, respectively.

For the signal PDF, we use the product of a Gaussian in M_{bc} and a double Gaussian in ΔE . We fix the parameters of these functions to values determined by MC simulation [15]. The continuum background PDF is taken as the product of shapes in M_{bc} and ΔE , which are assumed to be uncorrelated. These shapes are obtained from sideband events, with 0.1 GeV $< \Delta E < 0.2$ GeV for the M_{bc} function and with 5.20 GeV/ $c^2 < M_{bc} < 5.26$ GeV/ c^2 for the ΔE function, and are confirmed with a continuum MC sample. We use the following parametrization first used by the ARGUS collaboration [16], $f(M_{bc}) \propto M_{bc} \sqrt{1 - x^2} \exp[-\xi(1 - x^2)]$, to model the M_{bc} background, with x given by M_{bc}/E_{beam} and ξ as a fit parameter. The ΔE background shape is modeled by a first order polynomial whose slope is a fit parameter. The projections of the fit results are shown in Fig. 1 by solid curves. The fit yields are 217 ± 17 , $28.6^{+6.5}_{-5.8}$, and $48.8^{+8.2}_{-7.5}$ for the $p\bar{p}K^+$, $p\bar{p}K_S^0$, and $p\bar{\Lambda}\pi^-$ modes, respectively.

We study the proton angular distribution of the baryon-antibaryon pair system in its helicity frame. The angle θ_p is defined as the angle between the proton direction and the opposite of the light meson direction in the baryon-antibaryon pair rest frame. Note that after charge conjugation, the angle is determined by \bar{p} and K^+ (or p and K^-) for the $p\bar{p}K^+$ mode. Fig. 2(a)-(c) shows the branching fractions as a function of $\cos\theta_p$. The error bars include the statistical uncertainty from the fit and the systematic uncertainty. It is clear that the fragmentation process is favored for the $p\bar{p}K^+$ mode. Protons are emitted along the K^- direction most of the time, which can be explained by a parent $b \rightarrow s$ penguin transition followed by $s\bar{u}$ fragmentation into the final state. The $\cos\theta_p$ distribution of the $p\bar{p}K_S^0$ mode does not have enough statistics to support or refute this interpretation, although it seems to be peaked towards ± 1 since the flavor information is not applied in this case. The distribution for the $p\bar{\Lambda}\pi^-$ mode is quite flat, in contrast to that of the $p\bar{p}K^+$ mode,

although both presumably share a common origin in the $b \rightarrow s$ transition. In fact, this parentage suggests that it would be more suitable to draw the proton angular distribution of the $p\pi^-$ pair relative to the $\bar{\Lambda}$ direction; this is shown in Fig. 2(d). It is evident that the above interpretation is supported: the proton tends to emerge parallel to the $\bar{\Lambda}$ baryon. As a cross check, the distribution of $\cos\theta_p$ for background events in the $p\bar{p}K^+$ sample is shown in Fig. 2(e). (Similar distributions are obtained for the backgrounds of the $p\bar{p}K_S^0$ and $p\bar{\Lambda}\pi^-$ modes.) The background has a $1 + \cos^2\theta_p$ distribution, which can be explained as arising from the random combination of two high momentum particles from the $q\bar{q}$ jets. The fragmentation signature is not seen in the $B^+ \rightarrow J/\psi K^+$ mode, where the J/ψ meson decays to a $p\bar{p}$ pair. For J/ψ candidates with invariant mass in the range $3.07 \text{ GeV}/c^2 < M_{p\bar{p}} < 3.11 \text{ GeV}/c^2$, the distribution of $\cos\theta_p$ is flat, as shown in Fig. 2(f).

The differential branching fraction as a function of the baryon pair invariant mass is shown in Fig. 3. Here, the efficiency as a function of baryon pair mass for each signal mode is determined by MC simulation, with the events distributed uniformly in phase space. The regions $2.850 \text{ GeV}/c^2 < M_{p\bar{p}} < 3.128 \text{ GeV}/c^2$ and $3.315 \text{ GeV}/c^2 < M_{p\bar{p}} < 3.735 \text{ GeV}/c^2$ are excluded to remove background from B decay modes containing an η_c , J/ψ , ψ' , χ_{c0} , or χ_{c1} meson. The width of the low mass enhancement in each distribution of Fig. 3 depends on the signal mode. A different narrow width is seen also in the newly discovered $B^+ \rightarrow \Lambda\bar{\Lambda}K^+$ decay [17].

Systematic uncertainties are determined using high statistics control data samples. For proton identification, we use a $\Lambda \rightarrow p\pi^-$ sample, while for K/π identification we use a $D^{*+} \rightarrow D^0\pi^+$, $D^0 \rightarrow K^-\pi^+$ sample. Tracking efficiency is measured with fully and partially reconstructed D^* samples. The K_S^0 reconstruction efficiency is determined from a $D^- \rightarrow K_S^0\pi^-$ sample. The Λ and K_S^0 reconstruction efficiencies have the same uncertainty due to off-IP tracks if the uncertainty of the daughter proton identification criterion is not taken into account. The \mathcal{R} continuum suppression uncertainty is estimated from $b \rightarrow c$ control samples with similar final states. Based on these studies, we assign a 1% error for each track, 3% for each proton identification, 2% for each kaon/pion identification, 5% for K_S^0 and Λ off-IP reconstruction and 6% for the \mathcal{R} selection.

A systematic uncertainty of 4% in the fit yield is determined by varying the parameters of the signal and background PDFs. The MC statistical uncertainty and binning of the baryon pair mass contribute a 2% error in the branching fraction determination. The error on the number of $B\bar{B}$ pairs is 1%, where the assumption is made that the branching fractions of $\Upsilon(4S)$ to neutral and charged $B\bar{B}$ pairs are equal.

We first sum the correlated errors linearly and then combine with the uncorrelated ones in quadrature. The total systematic uncertainties are 11%, 12%, and 12% for the $p\bar{p}K^+$, $p\bar{p}K_S^0$, and $p\bar{\Lambda}\pi^-$ modes, respectively.

The newly observed narrow pentaquark state, Θ^+ [18], can decay into pK_S^0 . We perform a search in our data sample by requiring $1.53 \text{ GeV}/c^2 < M_{pK_S^0} < 1.55 \text{ GeV}/c^2$. The M_{bc} and ΔE projection plots in Fig. 4 show no evidence for a pentaquark signal. Since there are few events in the fit window, we fix the background shapes from side-band data. We use the fit results to estimate the expected background and compare this with the observed number of events in the signal region to set the upper limit on the yield [19, 20]. The systematic uncertainty is included in this estimation. The upper limit yield is determined to be 3.9 at the 90% confidence level. The related upper limit product of branching fractions is $\mathcal{B}(B^0 \rightarrow \Theta^+\bar{p}) \times \mathcal{B}(\Theta^+ \rightarrow pK_S^0) < 2.3 \times 10^{-7}$ at the 90% confidence level. We also perform a search for Θ^{++} , which can decay to pK^+ . Because there are only theoretical conjectures for

the existence of such a state, we examine the wider mass region of $1.6 \text{ GeV}/c^2 < M_{pK^+} < 1.8 \text{ GeV}/c^2$. We find no evidence for signal. Assuming this state is narrow and centered near $1.71 \text{ GeV}/c^2$, the upper limit yield is 3.3 events at the 90% confidence level. The related upper limit product of branching fractions is $\mathcal{B}(B^+ \rightarrow \Theta^{++}\bar{p}) \times \mathcal{B}(\Theta^{++} \rightarrow pK^+) < 9.1 \times 10^{-8}$ at the 90% confidence level.

One theoretical conjecture [6] suggests that a glueball resonance with mass near $2.3 \text{ GeV}/c^2$ may explain the $M_{p\bar{p}}$ threshold peaking behavior for the $p\bar{p}K^+$ mode. Since the $M_{p\bar{p}}$ mass resolution is about $10 \text{ MeV}/c^2$, we scan through the $2.2 \text{ GeV}/c^2 < M_{p\bar{p}} < 2.4 \text{ GeV}/c^2$ mass region with a $20 \text{ MeV}/c^2$ wide window. The highest upper limit yield is found to be 18.9. We use this data set to set an upper limit on the product of branching fractions of $\mathcal{B}(B^+ \rightarrow \text{glueball } K^+) \times \mathcal{B}(\text{glueball} \rightarrow p\bar{p}) < 4.1 \times 10^{-7}$ at the 90% confidence level for a possible narrow glueball state with mass in the $2.2 - 2.4 \text{ GeV}/c^2$ range. The theoretical prediction is around 1×10^{-6} .

In summary, using $152 \times 10^6 B\bar{B}$ events, we measure the angular and invariant mass distributions of the baryon-antibaryon pair system near threshold for the $p\bar{p}K^+$, $p\bar{p}K_S^0$ and $p\bar{\Lambda}\pi^-$ baryonic B decay modes. The quark fragmentation process is supported, but the gluonic picture is disfavored. Searches for a B meson decaying into pentaquark Θ^+ or a glueball in the above related modes give null results. We set stringent upper limits on the product of the decay branching fractions.

We thank the KEKB group for the excellent operation of the accelerator, the KEK Cryogenics group for the efficient operation of the solenoid, and the KEK computer group and the National Institute of Informatics for valuable computing and Super-SINET network support. We acknowledge support from the Ministry of Education, Culture, Sports, Science, and Technology of Japan and the Japan Society for the Promotion of Science; the Australian Research Council and the Australian Department of Education, Science and Training; the National Science Foundation of China under contract No. 10175071; the Department of Science and Technology of India; the BK21 program of the Ministry of Education of Korea and the CHEP SRC program of the Korea Science and Engineering Foundation; the Polish State Committee for Scientific Research under contract No. 2P03B 01324; the Ministry of Science and Technology of the Russian Federation; the Ministry of Education, Science and Sport of the Republic of Slovenia; the National Science Council and the Ministry of Education of Taiwan; and the U.S. Department of Energy.

* on leave from Nova Gorica Polytechnic, Nova Gorica

- [1] K. Abe *et al.* (Belle Collaboration), Phys. Rev. Lett. **88**, 181803 (2002).
- [2] M.Z. Wang, *et al.* (Belle Collaboration), Phys. Rev. Lett. **90**, 201802 (2003).
- [3] M.Z. Wang *et al.* (Belle Collaboration), Phys. Rev. Lett. **92**, 131801 (2004).
- [4] W.S. Hou and A. Soni, Phys. Rev. Lett. **86**, 4247 (2001).
- [5] C.K. Chua, W.S. Hou and S.Y. Tsai, Phys. Lett. **B528**, 233 (2002).
- [6] C. K. Chua, W. S. Hou and S. Y. Tsai, Phys. Lett. B **544**, 139 (2002).
- [7] J.L. Rosner, Phys. Rev. D **68**, 014004 (2003).
- [8] B. Kirbikov, A. Stavinsky, and V. Fedotov, Phys. Rev. C **69**, 055205 (2004).
- [9] J.Z. Bai *et al.* (BES Collaboration), Phys. Rev. Lett. **91**, 022001 (2003); J.Z. Bai *et al.* (BES Collaboration), hep-ex/0405050.
- [10] Throughout this report, inclusion of charge conjugate mode is always implied unless otherwise

stated.

- [11] S. Kurokawa and E. Kikutani *et al.*, Nucl. Instr. and Meth. A **499**, 1 (2003).
- [12] A. Abashian *et al.* (Belle Collaboration), Nucl. Instr. and Meth. A **479**, 117 (2002).
- [13] R.A. Fisher, Annals of Eugenics **7**, 179 (1936).
- [14] K. Abe *et al.* (Belle Collaboration), Phys. Lett. **B517**, 309 (2001).
- [15] There are small corrections applied to these parameters based on the study of the difference between data and MC of $B \rightarrow D\pi$ decays.
- [16] H. Albrecht *et al.*, Phys. Lett. **B241**, 278 (1990); *ibid.* **B254**, 288 (1991).
- [17] Y.J. Lee, *et al.* (Belle Collaboration), hep-ex/0406067.
- [18] T. Nakano *et al.* (LEPS Collaboration), Phys. Rev. Lett.**91**, 012002 (2003).
- [19] G.J. Feldman and R.D. Cousins, Phys. Rev. D **57**, 3873 (1998).
- [20] J. Conrad *et al.*, Phys. Rev. D **67**, 012002 (2003).

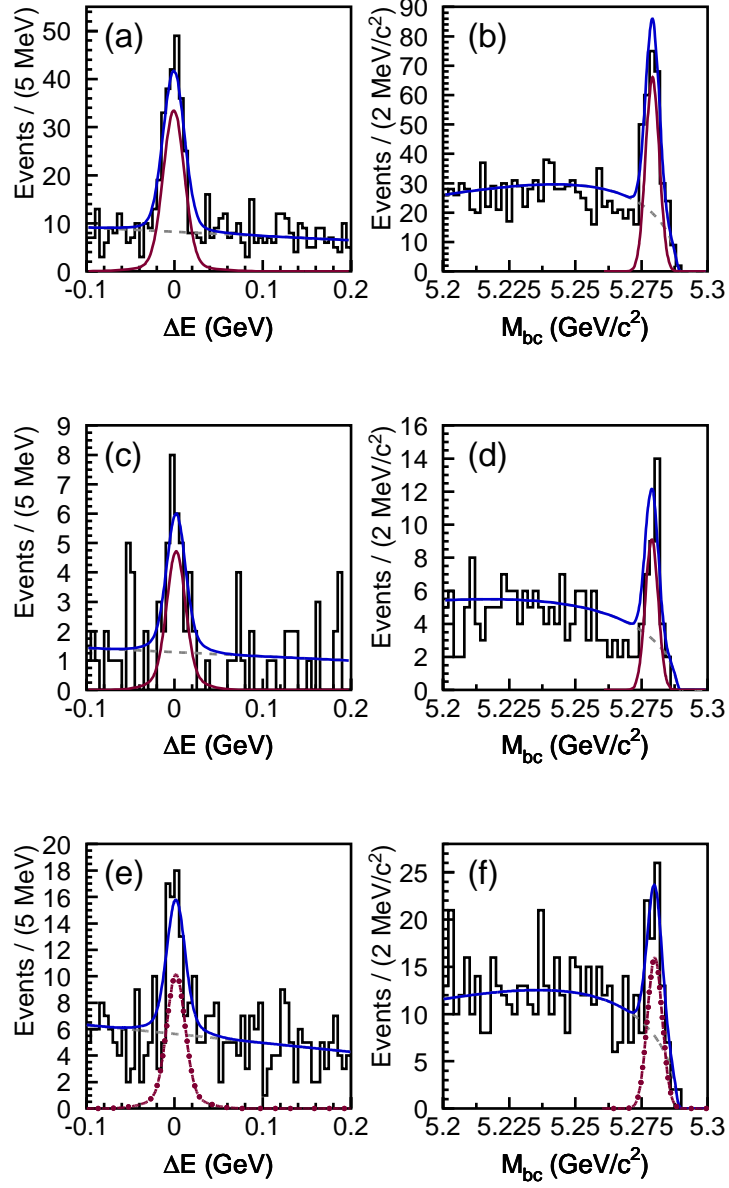


FIG. 1: Distributions of ΔE and M_{bc} , respectively, for (a) and (b) $p\bar{p}K^+$, (c) and (d) $p\bar{p}K_S^0$, and (e) and (f) $p\bar{\Lambda}\pi^-$ modes with baryon-antibaryon pair mass less than $2.85 \text{ GeV}/c^2$. The blue, red and dashed lines represent the combined fit result, fitted signal and fitted background, respectively.

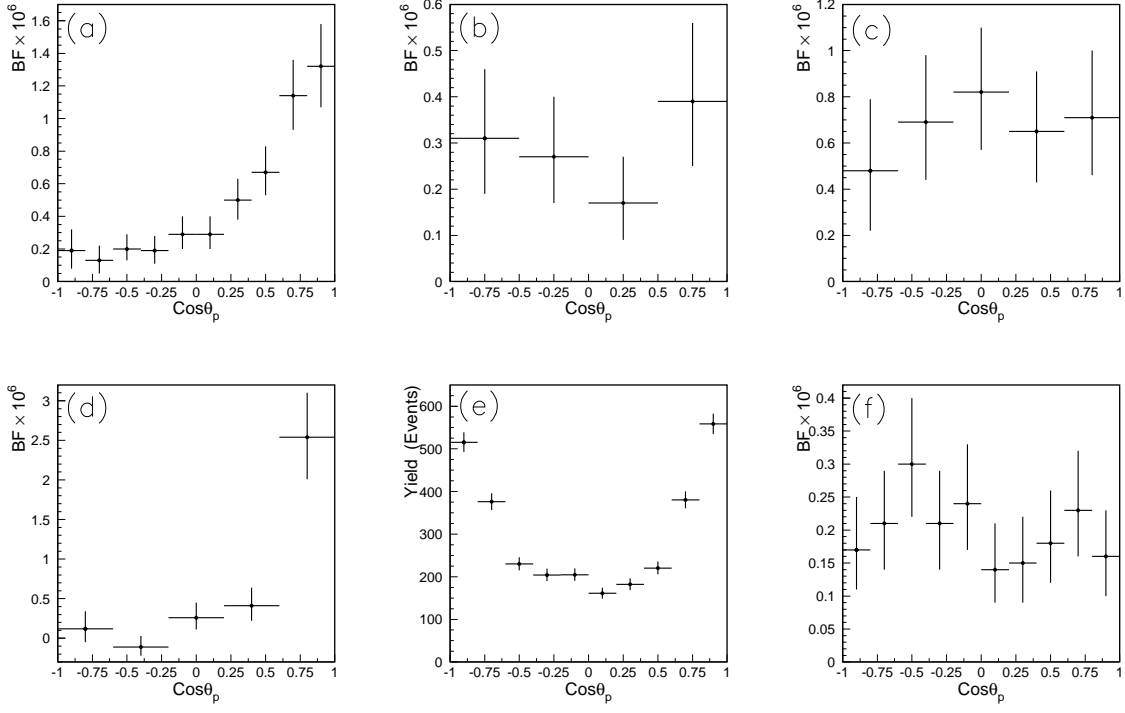


FIG. 2: Branching fraction *vs.* proton helicity angle in the baryon-antibaryon pair system for (a) $p\bar{p}K^+$, (b) $p\bar{p}K_S^0$, and (c) $p\bar{\Lambda}\pi^-$ modes. (d) The proton angular distribution of the $p\pi^-$ system against the $\bar{\Lambda}$ direction in the $p\bar{\Lambda}\pi^-$ mode. (e) Background yield of $p\bar{p}K^+$ in the fit. (f) Comparison with the J/ψ mass region.

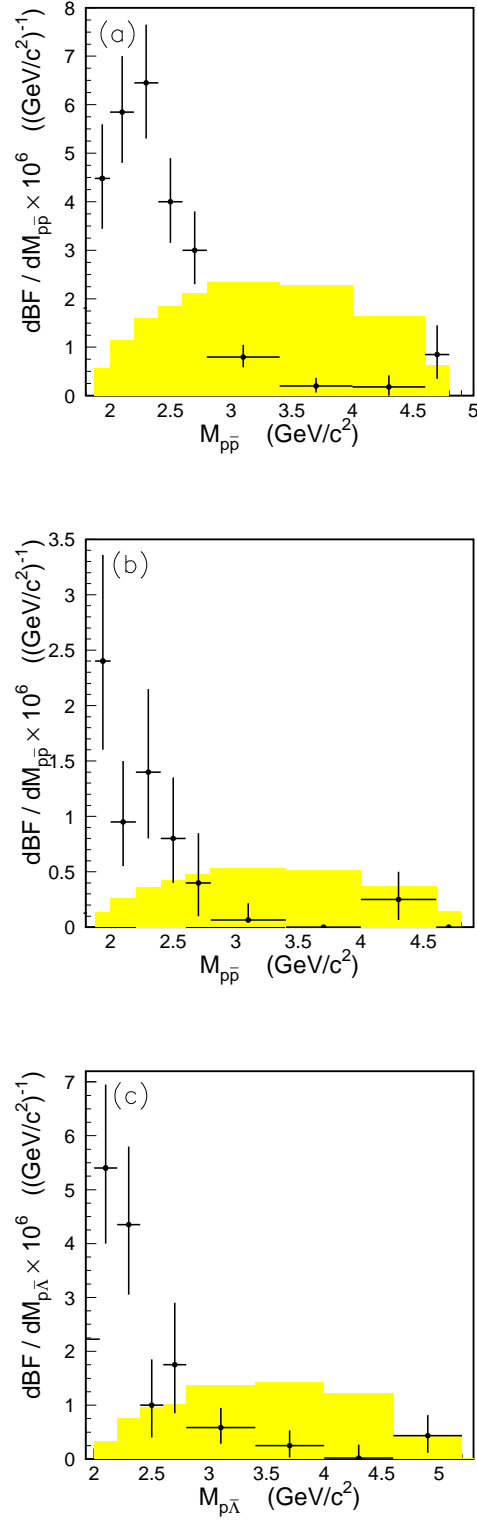


FIG. 3: Differential branching fraction for (a) $p\bar{p}K^+$, (b) $p\bar{p}K_S^0$, and (c) $p\bar{\Lambda}\pi^-$ modes as a function of baryon-antibaryon pair mass. The shaded distribution shows the expectation from a phase-space MC simulation with area scaled to the signal yield. A charmonium veto has been applied in (a) and (b).

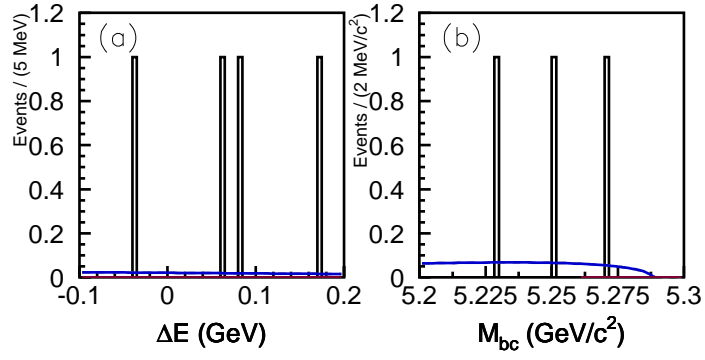


FIG. 4: Distributions of M_{bc} and ΔE for the $p\bar{p}K_S^0$ mode with $1.53 \text{ GeV}/c^2 < M_{pK_S^0} < 1.55 \text{ GeV}/c^2$. The curves represent the fit projections.